

AD-A125 020

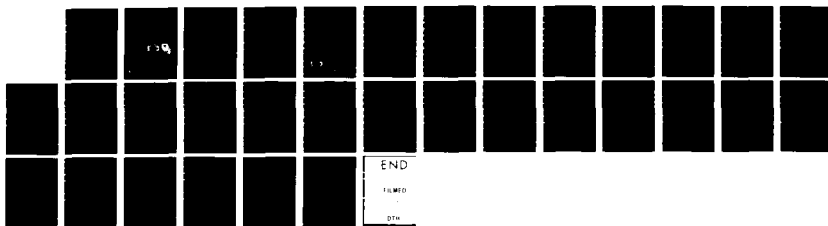
DISTRIBUTED SURVEILLANCE SYSTEMS(U) HARRY DIAMOND LABS
ADELPHI MD R N JOHNSON ET AL. NOV 82 HDL-TR-2006

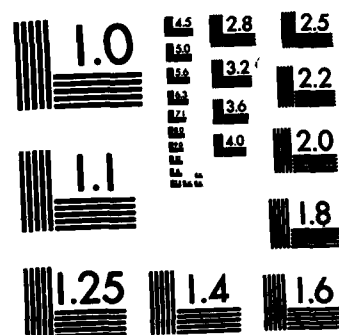
1/1

UNCLASSIFIED

F/G 9/2

NL





MICROCOPY RESOLUTION TEST CHART
NATIONAL BUREAU OF STANDARDS-1963-A

AD 775 204

October 1962

12

Distributed Surveillance Systems

by Richard M. Johnson
Benjamin E. Dunmore

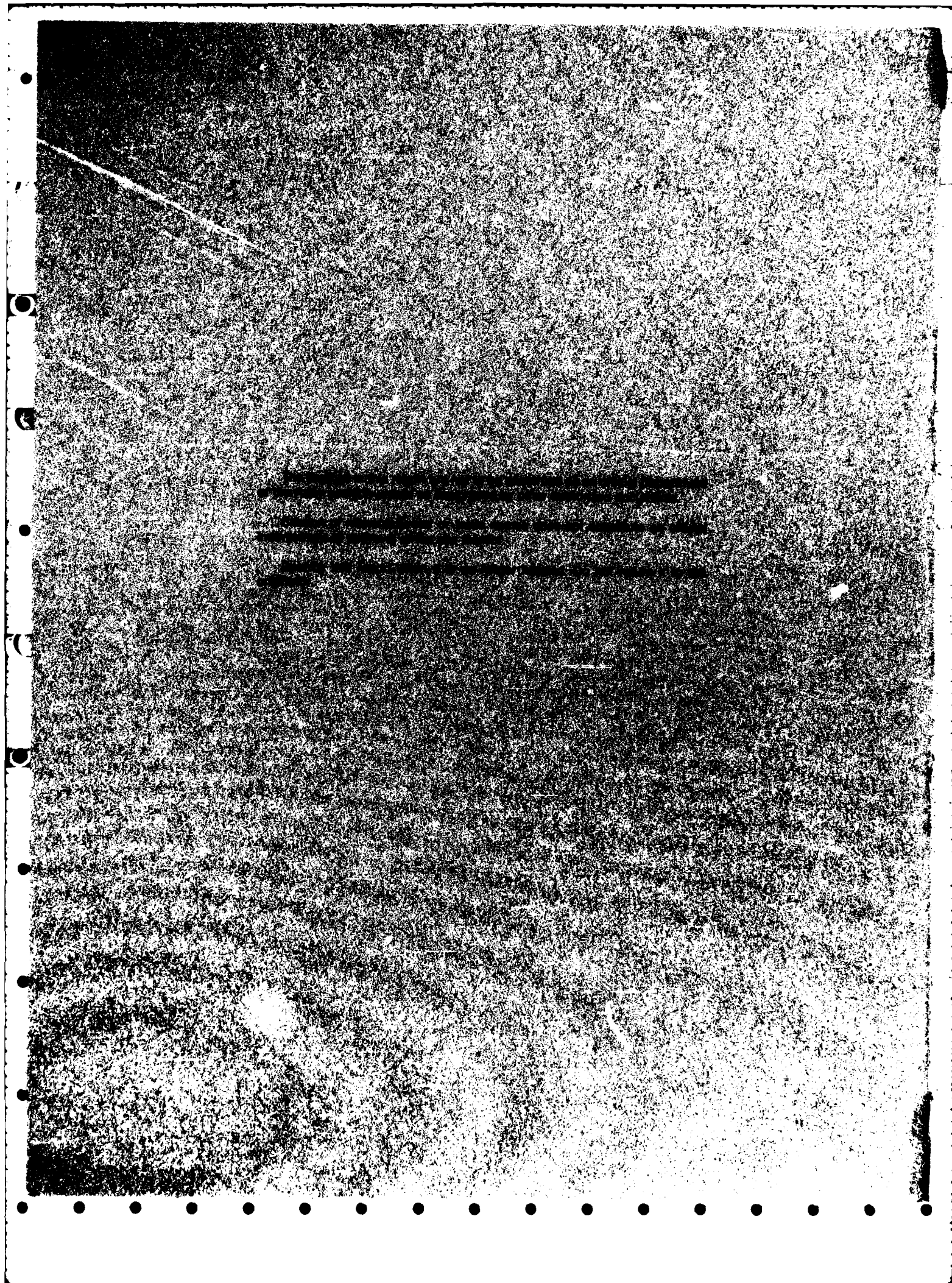
AD 775 204

AD 775 204

U.S. Army Research, Development
and Engineering Command
Fort Monmouth, New Jersey
August 1962

Approved for public release; distribution unlimited.

88 02 028 211



UNCLASSIFIED

SECURITY CLASSIFICATION OF THIS PAGE (When Data Entered)

REPORT DOCUMENTATION PAGE		READ INSTRUCTIONS BEFORE COMPLETING FORM
1. REPORT NUMBER HDL-TR-2006	2. GOVT ACCESSION NO. AD-A125 020	3. RECIPIENT'S CATALOG NUMBER
4. TITLE (and Subtitle) Distributed Surveillance Systems .		5. TYPE OF REPORT & PERIOD COVERED Technical Report ,
		6. PERFORMING ORG. REPORT NUMBER
7. AUTHOR(s) Richard N. Johnson Benjamin E. Dunmore		8. CONTRACT OR GRANT NUMBER(s)
9. PERFORMING ORGANIZATION NAME AND ADDRESS Harry Diamond Laboratories 2800 Powder Mill Road Adelphi, MD 20783		10. PROGRAM ELEMENT, PROJECT, TASK AREA & WORK UNIT NUMBERS Program Ele: 61102A
11. CONTROLLING OFFICE NAME AND ADDRESS U.S. Army Materiel Development and Readiness Command Alexandria, VA 22333		12. REPORT DATE November 1982
		13. NUMBER OF PAGES 33
14. MONITORING AGENCY NAME & ADDRESS (if different from Controlling Office)		15. SECURITY CLASS. (of this report) UNCLASSIFIED
		15a. DECLASSIFICATION/DOWNGRADING SCHEDULE
16. DISTRIBUTION STATEMENT (of this Report) Approved for public release; distribution unlimited.		
17. DISTRIBUTION STATEMENT (of the abstract entered in Block 20, if different from Report)		
18. SUPPLEMENTARY NOTES DRCMS Code: 611102H440011 DA: 1L161102AH44 HDL Project: A42252		
19. KEY WORDS (Continue on reverse side if necessary and identify by block number) Radar Sonar Multistatic Distributed Surveillance		
20. ABSTRACT (Continue on reverse side if necessary and identify by block number) * A distributed surveillance system comprises m sources and n sensors, each with varying degrees of autonomy, and a data-collection/processing center that exercises varying degrees of control over the system elements. The geometric aspects of distributed systems are examined, and the data-processing load/autonomy ratios of specific systems are evaluated. *		

DD FORM 1 JAN 79 1473 EDITION OF 1 NOV 65 IS OBSOLETE

UNCLASSIFIED

1 SECURITY CLASSIFICATION OF THIS PAGE (When Data Entered)

CONTENTS

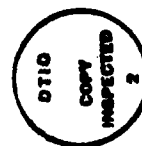
	<u>Page</u>
1. INTRODUCTION	5
2. NOTATIONS AND DEFINITIONS OF PARAMETERS	6
3. LOCATING SOURCES	6
4. LOCATING A SINGLE TARGET	13
5. SINGLE AUTONOMOUS SENSOR	15
6. REMOVAL OF CLOCK BIAS	18
7. REPORT SORTING FOR MULTIPLE-OBJECT DETECTIONS	22
8. DOPPLER FREQUENCY SHIFT DUE TO MOTION OF SOURCE	26
9. DISCUSSION	29
10. CONCLUSION	30
DISTRIBUTION	33

FIGURES

1. Distributed surveillance system (no target)	7
2. Distributed surveillance system (single target at position P_a)	13
3. Distributed surveillance system (single autonomous sensor P_k)	16
4. Distributed surveillance system (timing)	20
5. Multiple target detection dilemma	23
6. Range/time relationship	25
7. Doppler shifts due to motion of source	27

DTIC
ELECTE
S MAR 1 1983 **D**
B

3



Accession For	
NTIS GRA&I	<input checked="" type="checkbox"/>
DTIC TAB	<input type="checkbox"/>
Unannounced	<input type="checkbox"/>
Justification	
By _____	
Distribution/ _____	
Availability Codes	
Dist	Avail and/or Special
A	

1. INTRODUCTION

Types of distributed radar surveillance systems range from synthetic aperture radars (SAR's)¹ to netted systems of monostatic radars.² Two obvious discriminants for classifying this range of types are the amount of system coherence in the sensor signal processing and the degree of autonomy allowed the various elements. The SAR, which is certainly a distributed system (as a function of time), processes all sensor signals in a single coherent processor; however, the typical SAR can be viewed as a rigidly constrained (time) sequence of locations of monostatic radars. Thus, the "elements" of a SAR possess zero autonomy. The netted system of monostatic radars, wherein each radar ignores echo signals generated by all other radars, has no system coherence; in fact, the system discards or ignores potentially useful signals but allows an extreme autonomy of its various elements. An interesting feature of these two systems is the fact that the map produced by a SAR is self-registered and relatively independent of the path followed by the SAR; thus, only the relative precision of successive SAR locations is constrained. On the other hand, the netted radar system requires knowledge with absolute accuracy of the locations of all its elements.

Between these two extremes lie a number of interesting distributed surveillance systems whose configurations are pertinent to various tactical and strategic scenarios. Especially interesting are systems that can obtain precise target coordinates without the use of very narrow antenna beams, thus allowing some reduction in antenna size. Some of these systems are described and analyzed, in which time-interval measurements alone are sufficient to allow complete resolution of their geometry. While we intend only to address geometry, nongeometric radar facts will be brought to bear as needed to keep the systems realistic. For the systems studied here, it will be seen that precise, inaccurate (nonsynchronized) clocks suffice; a single benchmark (accurate location of an element in map coordinates) is adequate; and system coherence can be traded for data redundancy, just as coherent/incoherent signal processing can be traded off in a monostatic radar. An optimal exploitation of data redundancy is developed for each system.

¹John J. Kovaly, *Synthetic Aperture Radar*, Artech House (1976).

²Netted Radar Program, Volume II: TPS-5X Ground Surveillance Radar, MIT Lincoln Laboratory, contract F19628-80-C-0002 (30 September 1981).

2. NOTATIONS AND DEFINITIONS OF PARAMETERS

The following symbols are used in this report.

- (1) x, y, z Conventional Cartesian coordinates
- (2) j, k, a Integer subscripts identifying, respectively, (1) a distinct source at positions $P_j = x_j, y_j, z_j$; (2) a distinct sensor (receiver) at positions $P_k = x_k, y_k, z_k$, and (3) a distinct target at positions $P_a = x_a, y_a, z_a$. Integers m, n , and q are defined such that $0 < j < m$, $0 < k < n$, and $0 < a < q$.
- (3) C A central processing station at position $P_C = (x_C, y_C, z_C) = (0, 0, 0)$. A (one-way) communications link exists (where appropriate) from every sensor or transmitter position P_j to the central processing station.
- (4) T_{uv} A time interval multiplied by the speed of light (in meters per second) and read out in the system as slant range from position P_u to position P_v .
- (5) \vec{R}_{uv} A vector of magnitude $|\vec{R}_{uv}| = R_{uv} = T_{uv}$ from position P_u to position P_v .
- (6) A Absolute time measured from the beginning of the universe. Thus, the counter of a conventional cyclic clock will indicate $A(\text{modulo } M) + B$, where B is a bias in the clock count that has developed due to long-term drift, and M equals a full-scale (plus one count) state of the counter. Parameters A, M , and B are measured in meters and represent the distance a light pulse would travel during the clock periods represented by A, M , and B .
- (7) N A number indicated by a clock, i.e., the state of the clock-counter. A clock exists at each element of the system.

3. LOCATING SOURCES

In this and succeeding analyses of distributed surveillance systems, functional relations between various vectors, coordinates, and other parameters are presented in equation form. These equations are used to

establish sets of n linear vector equations in matrix format from which unknown coordinates and parameters can be determined.

Computations of coordinates x_j, y_j, z_j for the source(s) will be performed with reference to the notations and definitions presented above (see fig. 1). In this section, it is assumed that clocks at each element of the system are all mutually synchronized except for those in the source(s). Later it will be seen how the knowledge of sensor coordinates x_k, y_k, z_k and the synchronization of clocks can be determined.

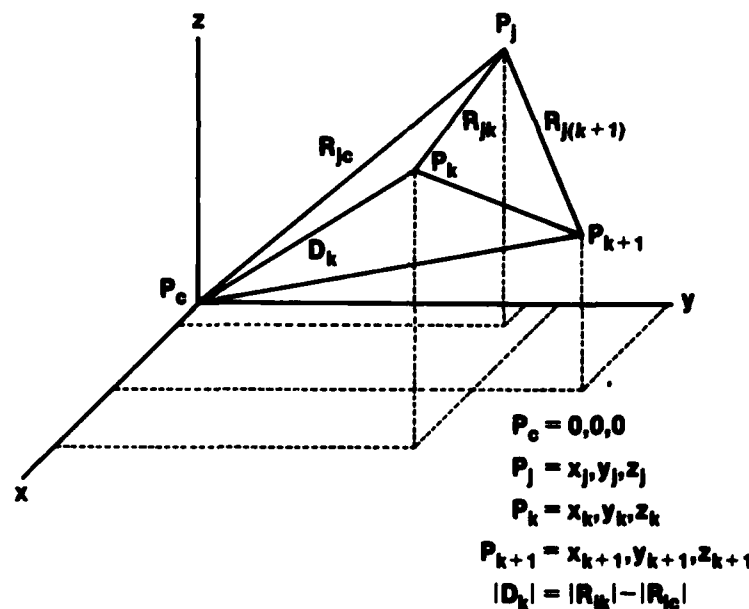


Figure 1. Distributed surveillance system (no target).

The absolute time of arrival, at sensor K , of a pulse emitted by source j is denoted as T_{jk} . Thus, $T_{jk} - T_{j(k+1)}$ is the difference in time of arrival at the k^{th} and $(k+1)^{\text{th}}$ sensors of a pulse emitted by source j . Each sensor reports the times, T_{jk} , to central processor C , where T_{jc} , the time of arrival at C of the pulse from source j , is available. In accordance with definition 5 above,

$$T_{jk} - T_{jc} = R_{jk} - R_{jc} = D_k \quad , \quad (1)$$

where R_{jk} is the distance in meters separating source j from sensor k , and R_{jc} is the distance separating source j from C .

Equation (1) will be used to derive a set of n linear equations in unknowns x_j , y_j , z_j , and R_{jc} . In order to accomplish this, a vector V with elements V_k is defined such that

$$\begin{aligned} V_1 &= (T_{j1} - T_{jc})^2 = D_1^2 \\ V_2 &= (T_{j2} - T_{jc})^2 = D_2^2 \\ &\quad \cdot \quad \cdot \quad \cdot \\ &\quad \cdot \quad \cdot \quad \cdot \\ &\quad \cdot \quad \cdot \quad \cdot \\ V_k &= (T_{jk} - T_{jc})^2 = D_k^2 \\ V_n &= (T_{jn} - T_{jc})^2 = D_n^2 \end{aligned} \quad (2)$$

The differences of adjacent vector elements are

$$\begin{aligned} V_1 - V_2 &= (T_{j1} - T_{jc})^2 - (T_{j2} - T_{jc})^2 \quad , \\ V_2 - V_3 &= (T_{j2} - T_{jc})^2 - (T_{j3} - T_{jc})^2 \quad , \\ &\quad \cdot \quad \cdot \quad \cdot \\ &\quad \cdot \quad \cdot \quad \cdot \\ &\quad \cdot \quad \cdot \quad \cdot \\ V_k - V_{k+1} &= (T_{jk} - T_{jc})^2 - (T_{j(k+1)} - T_{jc})^2 \quad , \\ &\quad \cdot \quad \cdot \quad \cdot \\ &\quad \cdot \quad \cdot \quad \cdot \\ &\quad \cdot \quad \cdot \quad \cdot \\ V_{n-1} - V_n &= (T_{j(n-1)} - T_{jc})^2 - (T_{jn} - T_{jc})^2 \quad . \end{aligned} \quad (3)$$

Expanding the k^{th} element of (3) gives

$$v_k - v_{k+1} = (T_{jk}^2 - T_{j(k+1)}^2) - 2T_{jc}(T_{jk} - T_{j(k+1)}) \quad , \quad (4)$$

which, in accordance with definition 5, becomes

$$v_k - v_{k+1} = R_{jk}^2 - R_{j(k+1)}^2 - 2R_{jc}(T_{jk} - T_{j(k+1)}) \quad . \quad (5)$$

It follows from the geometry in figure 1 that

$$R_{jk}^2 = (x_j - x_k)^2 + (y_j - y_k)^2 + (z_j - z_k)^2 \quad (6)$$

and

$$R_{j(k+1)}^2 = (x_j - x_{k+1})^2 + (y_j - y_{k+1})^2 + (z_j - z_{k+1})^2 \quad . \quad (7)$$

Also, since $x_c = y_c = z_c = 0$,

$$R_{ck}^2 = x_k^2 + y_k^2 + z_k^2 \quad (8)$$

and

$$R_{c(k+1)}^2 = x_{k+1}^2 + y_{k+1}^2 + z_{k+1}^2 \quad . \quad (9)$$

Furthermore, by equation (1),

$$T_{jk} - T_{j(k+1)} = D_k - D_{k+1} \quad . \quad (10)$$

Combining equations (5) to (10) and collecting terms in the unknown quantities x_j , y_j , z_j , and R_{jc} gives

$$2(x_{k+1} - x_k)x_j + 2(y_{k+1} - y_k)y_j + 2(z_{k+1} - z_k)z_j \quad (11)$$

$$+ 2(D_{k+1} - D_k)R_{jc} = [v_k - v_{k+1} + (R_{c(k+1)}^2 - R_{ck}^2)] \quad .$$

$$2 \begin{vmatrix} (x_2 - x_1) & (y_2 - y_1) & (z_2 - z_1) & (D_2 - D_1) \\ \cdot & \cdot & \cdot & \cdot \\ (x_{k+1} - x_k) & (y_{k+1} - y_k) & (z_{k+1} - z_k) & (D_{k+1} - D_k) \\ \cdot & \cdot & \cdot & \cdot \\ (x_n - x_{n-1}) & (y_n - y_{n-1}) & (z_n - z_{n-1}) & (D_n - D_{n-1}) \end{vmatrix} \begin{vmatrix} x_j \\ y_j \\ z_j \\ R_{jc} \end{vmatrix} = \begin{vmatrix} (v_1 - v_2 + R_{c2}^2 - R_{c1}^2) \\ \cdot & \cdot & \cdot \\ (v_k - v_{k+1} + R_{c(k+1)}^2 - R_{ck}^2) \\ \cdot & \cdot & \cdot \\ (v_{n-1} - v_n + R_{cn}^2 - R_{c(n-1)}^2) \end{vmatrix} \quad (13)$$

If n exceeds 4 in equation (13), an overconstrained set of equations exists, and it is almost impossible to conceive of a single vector (x_j, y_j, z_j, R_{jc}) that when multiplied by the row vectors of the matrix in (13) would give precisely the measured values in the vector on the right side of (13). Clearly, some estimated vector (x_j, y_j, z_j, R_{jc}) is required that fits the v le data set in the measurement vector. Equation (13) can be written in the compact symbolic matrix format

$$2[A][J] = [B]$$

or

$$2AJ = B \quad .$$

The solution requires a guess vector, G , such that

$$2AG = C \quad .$$

However, this produces an error vector

$$E = C - b \quad ,$$

the elements of which must be minimized in some fashion. Gauss solved this problem, using the criterion that the sum of squared elements of E is minimized. To see how this was done, note that

$$E^2 = E_T E ,$$

where E_T is the transpose of the vector E . Thus,

$$E_T E = (2AG - B)_T (2AG - B) .$$

Differentiating partially with respect to G gives

$$\begin{aligned} \frac{\partial (E_T E)}{\partial G} &= 2A_T (2AG - B) + (2AG - B)_T 2A \\ &= 2A_T (2AG - B) + 2A_T (2AG - B) \\ &= 8A_T AG - 4A_T B . \end{aligned}$$

Equating this derivative to zero provides the desired result:

$$2A_T AG = A_T B . \quad (14)$$

The matrix $A_T A$ is a square, 4×4 nonsingular matrix. Thus, equation (14) provides a unique solution for G , independent of the number of sensors. The solution for G may be inserted into equation (13), and the guess vector $2AG = C$ allows the evaluation of $C - B$ as a check on the overall system. If it is found that two adjacent elements of $C - B$ are unduly large, then it may be concluded that the sensor with clock readings common to these two elements has been mislocated, or has a clock malfunction, etc.

Further discussion of the matrix $[A]$ is appropriate at this point. The first three column vectors of $[A]$ represent static data so long as no sensors are moved; thus, only the fourth column vector of $[A]$ contains real-time (pulse-to-pulse) information. If the distance between each sensor and C could somehow be directly measured, then $[A]$ would become a three-column matrix, and $A_T A$, along with its inverse, could be precomputed just once for all sources or source positions, thus

reducing the real-time computation load by a considerable factor. The implications of this fact will be developed at a later point in the discussion.

4. LOCATING A SINGLE TARGET

Before we discuss system-target geometry, we should point out that, in general, we are no longer discussing single-pulse timing. If there were no clutter, and if each target were large enough in radar cross section to bring its echo clear of thermal noise in the receivers, then we could proceed pulse by pulse. Since clutter is present and targets are small, it is required that each sensor have some target-detection mechanism that separates meaningful targets from clutter, reporting the average clock reading that corresponds to each target's position, P_a . Clearly, if there is to be motion of the source(s), the requirement is that the target-detection interval at each sensor be short enough to make source motion during each interval negligible.

Assume now that (a) the system is as described in the previous section and (b) the location of the source(s) is now known (see fig. 2). A single target, A, is added at position $P_a (x_a, y_a, z_a)$ with unobstructed line of sight from the target to the source(s) and sensor(s). Assume further that each sensor detects the target after receiving a sequence of echos due to one sequence of illumination pulses from source j . Each sensor then sends a clock reading to the central processor, C, that represents the total distance from P_j to P_k via P_a .

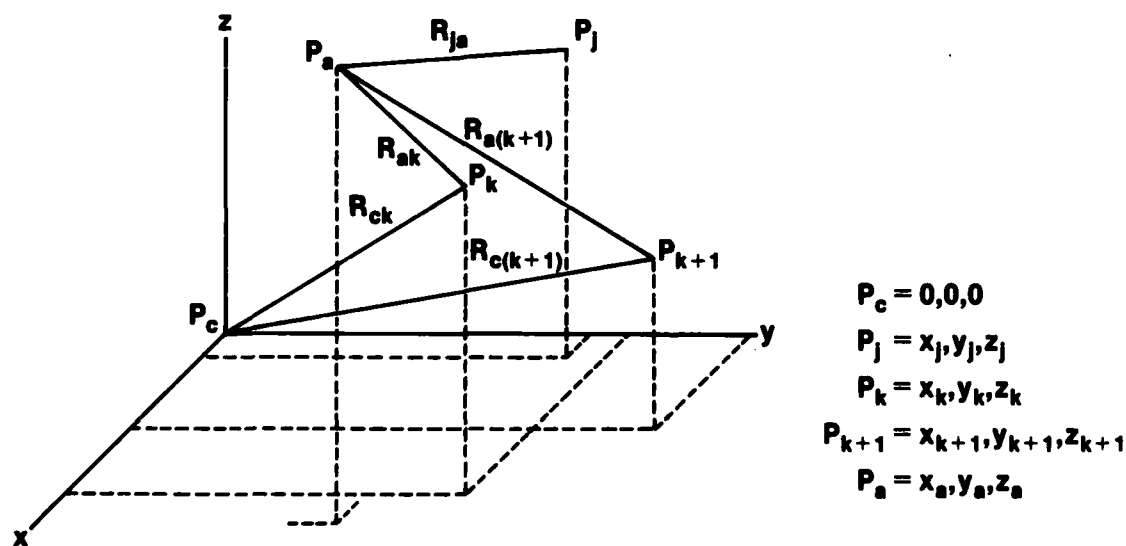


Figure 2. Distributed surveillance system (single target at position P_a).

This distance is $R_{ja} + R_{ak}$. At position C, each reading is squared and a vector, B_k , of successive differences of these squares is formed. Thus

$$\begin{aligned} B_k &= (R_{ja} + R_{a(k+1)})^2 - (R_{ja} + R_{ak})^2 \\ &= 2R_{ja}(R_{a(k+1)} - R_{ak}) + R_{a(k+1)}^2 - R_{ak}^2 \end{aligned} \quad (15)$$

The term $2R_{ja}(R_{a(k+1)} - R_{ak})$ comprises the unknown R_{ja} and twice the difference between two knowns, $R_{a(k+1)}$ and R_{ak} . This difference in terms of attendant coordinates at positions P_a , P_k , and P_{k+1} is obtainable from

$$\begin{aligned} R_{a(k+1)}^2 - R_{ak}^2 &= (x_a - x_{k+1})^2 + (y_a - y_{k+1})^2 + (z_a - z_{k+1})^2 \\ &\quad - [(x_a - x_k)^2 + (y_a - y_k)^2 + (z_a - z_k)^2] \end{aligned}$$

In this equation, we may substitute

$$R_{C(k+1)}^2 - R_{Ck}^2 = (x_{k+1}^2 + y_{k+1}^2 + z_{k+1}^2) - (x_k^2 + y_k^2 + z_k^2) ,$$

thus

$$\begin{aligned} R_{a(k+1)}^2 - R_{ak}^2 &= R_{C(k+1)}^2 - R_{Ck}^2 - 2(x_{k+1} - x_k)x_a \\ &\quad - 2(y_{k+1} - y_k)y_a - 2(z_{k+1} - z_k)z_a \end{aligned} \quad (16)$$

Combining equations (15) and (16) and collecting terms in all unknowns x_a , y_a , z_a , and R_{ja} gives

$$\begin{aligned} 2(x_{k+1} - x_k)x_a + 2(y_{k+1} - y_k)y_a + 2(z_{k+1} - z_k)z_a - 2(R_{a(k+1)} - R_{ak})R_{ja} \\ = R_{C(k+1)}^2 - R_{Ck}^2 - B_k \end{aligned} \quad (17)$$

Equation (17) can be written successively for the cases $K = 1, 2, \dots, k, \dots, n$, thus yielding the matrix equation

$$2 \begin{vmatrix} (x_2 - x_1) & (y_2 - y_1) & (z_2 - z_1) & (R_{a1} - R_{a2}) \\ \cdot & \cdot & \cdot & \cdot \\ \cdot & \cdot & \cdot & \cdot \\ (x_{k+1} - x_k) & (y_{k+1} - y_k) & (z_{k+1} - z_k) & (R_{ak} - R_{a(k+1)}) \\ \cdot & \cdot & \cdot & \cdot \\ \cdot & \cdot & \cdot & \cdot \\ (x_n - x_{n-1}) & (y_n - y_{n-1}) & (z_n - z_{n-1}) & (R_{a(n-1)} - R_{an}) \end{vmatrix} \begin{vmatrix} x_a \\ y_a \\ z_a \\ R_{ja} \end{vmatrix} =$$

$$\begin{vmatrix} (R_{C2}^2 - R_{C1}^2 - B_1) \\ \cdot \\ \cdot \\ (R_{C(k+1)}^2 - R_{Ck}^2 - B_k) \\ \cdot \\ \cdot \\ (R_{Cn}^2 - R_{C(n-1)}^2 - B_{n-1}) \end{vmatrix} \quad (18)$$

This matrix equation can be solved by the methods used previously in solving equation (13).

Note here that the matrix of known values in equation (18) differs from the matrix of (13) only in the fourth column. Also, if the range from the source to the target, R_{ja} , were known by direct measurement, then, analogous to the source-location task, the real-time computation load would diminish considerably.

5. SINGLE AUTONOMOUS SENSOR

Harking back to the system described in section 4, a single roving sensor is now postulated that contains all the computing power of

central processor C and also "knows" its own location in absolute map coordinates at all times (see fig. 3). If the successive (known) positions of this sensor are labeled x_k, y_k, z_k ($1 \leq k \leq n$), then after all n positions have been occupied by this roving sensor, a computation can be made, as in section 3, to determine the relative locations of the sources. In this case $T_{jk} = D_f$ is substituted for $T_{jk} - T_{jc} = D_k$. Since $T_{jc} = R_{jc}$ no longer enters into the computation, the fourth column of the matrix in equation (13) is not required in the computations.

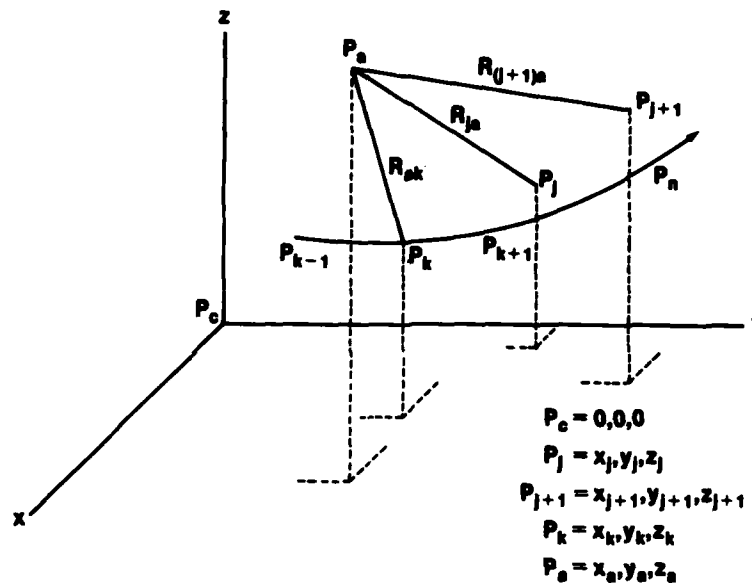


Figure 3. Distributed surveillance system (single autonomous sensor P_k).

Having thus determined the matrix of relative source locations, we may assume some favorable (known) vantage position for seeking out targets. Once again, if a single target is assumed, then for each source j a separate clock reading of $T_{ja} + T_{ak} = R_{ja} + R_{ak} = F_j$ will be obtained. Computing much as before, we find

$$F_{j+1}^2 - F_j^2 = R_{(j+1)a}^2 - R_{ja}^2 + 2R_{ak}(R_{(j+1)a} - R_{ja})$$

where

$$\begin{aligned}
R_{(j+1)a}^2 - R_{ja}^2 &= x_{j+1}^2 - x_j^2 - 2x_a(x_{j+1} - x_j) \\
&+ y_{j+1}^2 - y_j^2 - 2y_a(y_{j+1} - y_j) \\
&+ z_{j+1}^2 - z_j^2 - 2z_a(z_{j+1} - z_j) \quad .
\end{aligned}$$

Here, the matrix equation requiring solution is

$$2 \begin{vmatrix} (x_2 - x_1) & (y_2 - y_1) & (z_2 - z_1) & (R_{1a} - R_{2a}) \\ \cdot & \cdot & \cdot & \cdot \\ \cdot & \cdot & \cdot & \cdot \\ (x_{j+1} - x_j) & (y_{j+1} - y_j) & (z_{j+1} - z_j) & (R_{ja} - R_{(j+1)a}) \\ \cdot & \cdot & \cdot & \cdot \\ \cdot & \cdot & \cdot & \cdot \\ (x_n - x_{n-1}) & (y_n - y_{n-1}) & (z_n - z_{n-1}) & (R_{(n-1)a} - R_{na}) \end{vmatrix} \begin{vmatrix} x_a \\ y_a \\ z_a \\ R_{ak} \end{vmatrix} = \begin{vmatrix} (F_2^2 - F_1^2 + R_1^2(2)) \\ \cdot \\ \cdot \\ (F_{j+1}^2 - F_j^2 + R_j^2(j+1)) \\ \cdot \\ \cdot \\ (F_n^2 - F_{n-1}^2 + R_{(n-1)}^2(n)) \end{vmatrix} \quad (19)$$

The solution is carried out as in the previous systems. Note that each of n independent autonomous sensors can independently exploit a field of sources in this manner, and the additional cost of replicating the computing power of C --and its ability to determine its own location--may well be overcome by the fact that these sensors can be utterly passive.

6. REMOVAL OF CLOCK BIAS

The initial deployment of a distributed system might be accomplished in a number of ways. Conceptually, the easiest deployment would use benchmarks that have been accurately surveyed on the ground; however, a system that required such a survey would be severely limited in its range of applications. There is a technique that allows both self-established deployment and continual monitoring of incremental modifications to accommodate the expected flux of a battlefield situation. Since this technique can establish only the relative locations of the system elements, one is required, as might be expected, to know the absolute location (map coordinates) and orientation (north) of at least one element of the system. For ease of discussion, assume that the central processing element (P_C) is the one whose map coordinates and orientation are known. A high-resolution three-dimensional radar is placed at C, and used to determine the pulse source positions, P_j .

Consider m pulse source positions P_j , $0 \leq j \leq m$; receiver positions $0 \leq k \leq n$; and a central processing position P_C . Clocks exist at all positions with the following characteristics:

(a) All clocks have "identical" crystal-controlled frequency sources.

(b) Every clock has a b -bit counter, automatically recycling to a zero count after each $2(\exp b)$ cycles of its frequency source; thus, the clock counters have modulus $M = 2(\exp b)$

(c) Each clock has a bias B :

clock at P_j has bias B_j ,

clock at P_k has bias B_k ,

clock at P_C has bias B_C .

Assume that all sources have the same interpulse interval, and that this interval is equal to the modulus M of the clock counters. Modulus M is selected large enough to avoid ambiguous ranging and troublesome second-time-around echos. Finally, assume that each receiver can uniquely determine the identity of the source of each pulse it receives.

Each source emits a pulse as its clock recycles to zero; thus, source j will emit a pulse at $N_j = 0$ and $A_j = gM - B_j$, where g is some integer. This pulse will be received at C at time $A_C = gM - B_j + T_{jc}$, and the count N_{Cj} will be noted as $T_{jc} - B_j + B_C = N_{Cj}$. The same pulse will be received at receiver k at $A_k = gM - B_j + T_{jk}$, and the count N_{kj}

will be noted as $T_{jk} + B_k - B_j = N_{kj}$. Assuming that all P_j are known at C and that $T_{jc} = R_{jc}$, we have, for each pulse at C,

$$N_{cj} - R_{jc} = B_c - B_j \quad . \quad (20)$$

It is assumed that the numbers N_k as measured at the receivers are somehow transmitted to C (e.g., by laser, line of sight, telephone lines, and so on), not necessarily in real time.

This allows the further computation

$$N_{kj} - (N_{cj} - R_{jc}) = T_{jk} + B_k - B_c = R_{jk} - B_c + B_k \quad . \quad (21)$$

An examination of figure 4 shows that, so long as no single time interval exceeds M, and so long as all time computations are performed modulo M, these timing equations are correct, regardless of the magnitudes of the biases. At C, the analysis proceeds with the determination of the relative locations of all receivers and the clock biases. The computations are

$$L = (R_{jk} + B_k - B_c)^2 = R_{jk}^2 + B_k^2 + B_c^2 + 2B_k R_{jk} - 2B_c B_k - 2B_c R_{jk} \quad , \quad (22)$$

$$M = (R_{(j+1)k} + B_k - B_c)^2 = R_{(j+1)k}^2 + B_k^2 + B_c^2 + 2B_k R_{(j+1)k} - 2B_c B_k - 2B_c R_{(j+1)k} \quad , \quad (23)$$

$$N = (R_{j(k+1)} + B_{k+1} - B_c)^2 = R_{j(k+1)}^2 + B_{k+1}^2 + B_c^2 + 2B_{k+1} R_{j(k+1)} - 2B_c B_{k+1} - 2B_c R_{j(k+1)} \quad , \quad (24)$$

$$P = (R_{(j+1)(k+1)} + B_{k+1} - B_c)^2 = R_{(j+1)(k+1)}^2 + B_{k+1}^2 + B_c^2 + 2B_{k+1} R_{(j+1)(k+1)} - 2B_c B_{k+1} - 2B_c R_{(j+1)(k+1)} \quad , \quad (25)$$

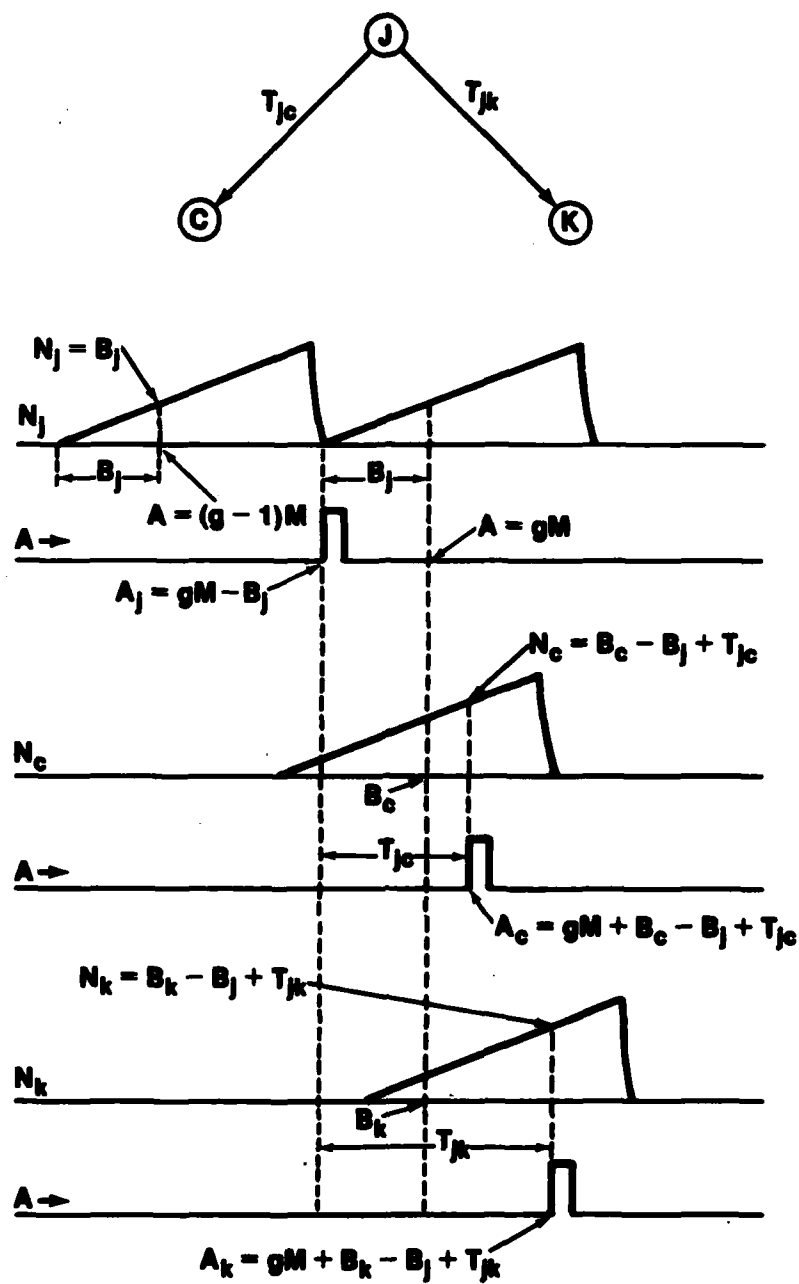


Figure 4. Distributed surveillance system (timing).

$$M - L = R_{(j+1)k}^2 - R_{jk}^2 + 2(B_k - B_c)(R_{(j+1)k} - R_{jk}) \quad , \quad (26)$$

and

$$\begin{aligned} P - L = & R_{(j+1)(k+1)}^2 - R_{j(k+1)}^2 \\ & + 2(B_{k+1} - B_c)(R_{(j+1)(k+1)} - R_{j(k+1)}) \quad . \end{aligned} \quad (27)$$

Here, the coefficients of $B_k - B_c$ and $B_{k+1} - B_c$ are known via direct measurement, for

$$R_{(j+1)k} - B_c + B_k - (R_{jk} - B_c + B_k) = R_{(j+1)k} - R_{jk}$$

and

$$\begin{aligned} R_{(j+1)(k+1)} - B_c + B_{k+1} - (R_{j(k+1)} - B_c + B_{k+1}) \\ = R_{(j+1)(k+1)} - R_{j(k+1)} \quad . \end{aligned}$$

Moreover,

$$\begin{aligned} [P - N] - [M - L] = \\ 2(x_k - x_{k+1})(x_{j+1} - x_j) + 2(y_k - y_{k+1})(y_{j+1} - y_j) \\ + 2(z_k - z_{k+1})(z_{j+1} - z_j) + 2(B_{k+1} - B_c)(R_{(j+1)(k+1)} - R_{j(k+1)}) \\ + 2(B_c - B_k)(R_{(j+1)k} - R_{jk}) \quad . \end{aligned} \quad (28)$$

The left side of this equation comprises terms that are computed solely from the various time measurements reported by the system. The right side contains two clock bias terms, each with a known coefficient, and the products of like Cartesian coordinates of source-to-source distances with sensor-to-sensor distances. Clearly, if we know five or more of either set of distances, we have a solvable set of equations for the unknown distance intervals.

The foregoing technique can be readily applied to the case of a single roving sensor that contains all the computational power of the system, if we require that this sensor have knowledge of its own position in map coordinates at all times, and constrain the sources to be immobile at (initially) unknown positions P_j .

This sensor will record its own clock states N_{jk} at a sequence of known positions $P_k (x_k, y_k, z_k)$. As before, each source emits a pulse at $N_j = 0$ and at $A_j = gM - B_j$. These are received at $A_{kj} = gM - B_j + T_{jk}$, and the state will be recorded as

$$N_{kj} = T_{jk} - B_j + B_k \quad . \quad (29)$$

Recall now that B_k is the bias of the clock in the single roving sensor; thus, it will not vary as location P_k is varied. Substituting B_c for B_k in this equation gives

$$N_{kj} = T_{jk} + B_j + B_c = R_{jk} - B_j + B_c \quad . \quad (30)$$

This equation is of the same form as equation (21) except for the change in sign of B_c , the fact that $-B_j$ is involved rather than $\pm B_k$, and the fact that the P_k rather than the P_j are now known. It should be clear that the analysis can proceed as with equation (19), with known and unknown position coordinates interchanged, and with biases B_j rather than B_k .

Having determined the relative positions of the sources, and the biases of their clocks relative to its own clock, we may program the single autonomous sensor to continually monitor the direct-path signals from these sources to correct for further changes in any clock biases. Similarly, clock biases in the multisensor arrangement with a central clock can be continually monitored and corrected.

7. REPORT SORTING FOR MULTIPLE-OBJECT DETECTIONS

In the systems so far discussed, angular measurements have been unnecessary. Only the best and most easily attainable aspect of electromagnetic surveillance techniques have been used to achieve the accuracy of position location desired. There is at least one application that requires only this measurement of time: range

instrumentation for tracking the location of one or more cooperative sources. The multiple sensor case is ideal for this task, if at least one nonmoving source is retained to allow tracking of the sensors' clock biases.

The more general application, where noncooperative moving objects must be detected and located, requires angular measurements to some degree for two reasons: the first is a practical radar consideration involving clutter levels, and the second is the report-sorting problem. Figure 5 depicts the dilemma of any of our systems when confronted by more than one detection. Assume objects A and B lie on isochrons for sensors k and $k + 1$ as shown. Each sensor will report two detections at clock states corresponding to the appropriate isochron. The central processor can now associate the reported clock states in a fashion that indicates objects at C and D, as well as at A and B. Additional sensors will, of course, provide additional data in more than sufficient quantity to resolve the simple ambiguity indicated in figure 5, but consider the processing load. If m sensors have each reported n distinct detections, the central processor has n^m possible combinations to sort through.

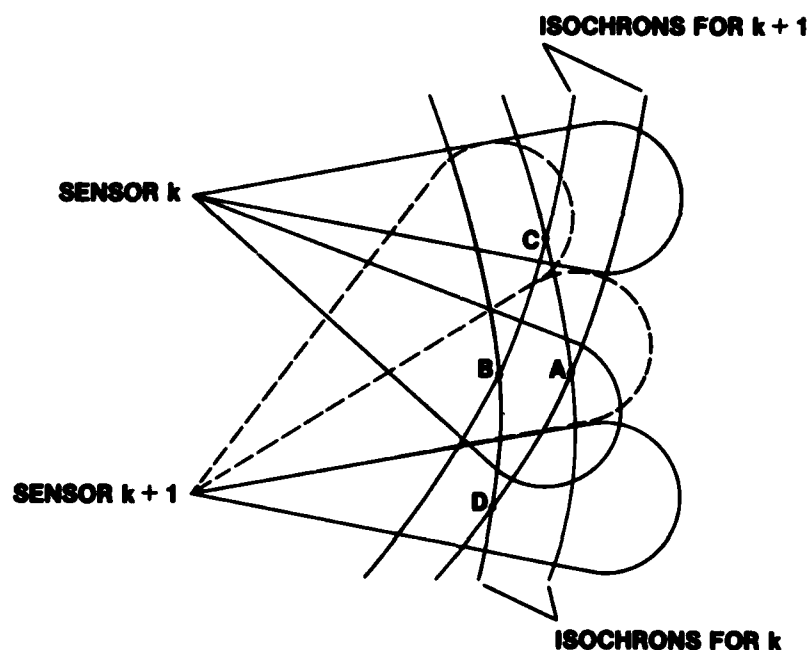


Figure 5. Multiple target detection dilemma.

Figure 5 shows sensors k and $k + 1$ with multiple simultaneous antenna beams. In the situation depicted, these antenna beams resolve the ambiguity, for each sensor now reports both the clock state and receiving beam identity for each detection. We note in passing that the antenna beam orientation of each sensor is approximately deducible at the central processor, since the direct-path geometry is known. Since angle measurement is not being used to establish positions of objects, but only to reduce ambiguities, an approximate knowledge of sensor orientation is adequate.

The architecture of the report-sorting mechanism is strongly affected by certain practical system considerations. Each sensor will have as few antenna beams as possible, so that the computational complexity of the antenna beam former is minimized. In most cases, for objects on the ground, clutter-level considerations will dictate the irreducible minimum of antenna beams required. One parameter of the system that will be fixed by the choice of angular resolution is the total integration time for detection at each sensor. The maximum autonomy of sensors is desired; therefore, it will be assumed that the integration epochs at the sensors are not mutually synchronized. This means that the central processor can never be assured that it has a complete static data set for any given object; moreover, the elements of the data set for a given object will have an age variation on the order of the integration interval, and, of course, many objects will not be detected by all sensors. Finally, for full exploitation of the system possibilities, each sensor must have a reasonably high false-detection probability. To deal with these and other complicating factors to be elucidated, the surveillance area shall be divided into cells centered at x_m, y_n, z_p . For each such cell, a memory and processing capability shall be provided. Since the customary echo-ranging range/time equation does not apply, we must compute, for each sensor/source/antenna-beam combination, the appropriate range/time relationship. Figure 6 shows one possible technique. For ease of explanation, a horizontal plane is considered in this figure. Positions P_j, P_k and ranges $R_{jk}, R_{ja} + R_{ak}$ are known, as well as the approximate beam angle A . It is desired to classify the reported $R_{ja} + R_{ak}$ according to the x_m, y_n cell(s) it may fit into; thus, the following computations are needed:

$$x_m = R_{ak} \cos A + x_k \quad , \quad (31)$$

$$y_n = R_{ak} \sin A + y_k \quad . \quad (32)$$

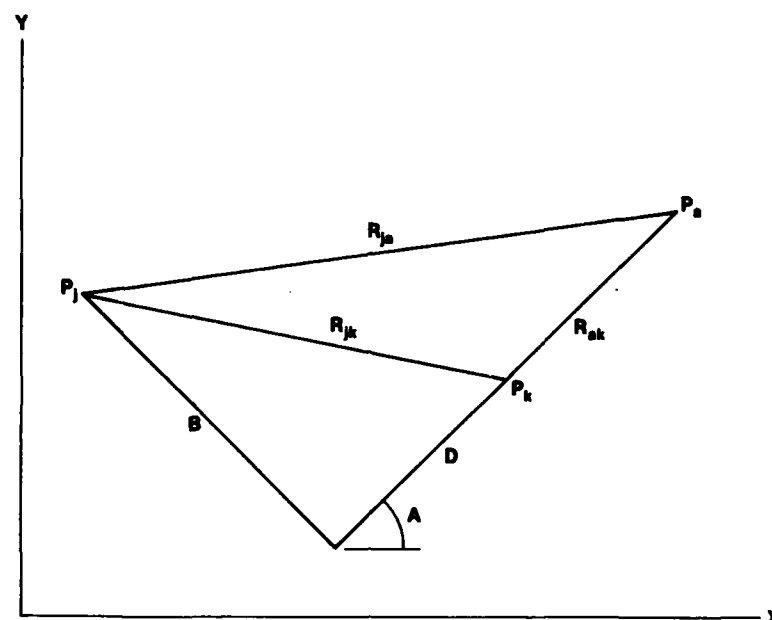


Figure 6. Range/time relationship.

Clearly R_{ak} must be found as a function of $R_{ak} + R_{ja}$. Constructing lines B and D, we can write

$$B \sin A + D \cos A = x_k - x_j \quad , \quad (33)$$

$$B \cos A - D \sin A = y_j - y_k \quad . \quad (34)$$

These two equations in B and D are readily solved for each beam of each sensor/source combination. Having solved for B and D, proceed as follows:

(a) Divide the square of B by $D + R_{ja} + R_{ak}$, and add $D + R_{ja} + R_{ak}$ to the quotient. Label the result E:

$$\frac{B^2}{R_{ja} + R_{ak} + D} + R_{ja} + R_{ak} + D = E \quad .$$

(b) Show that $E = 2R_{ja}$ by considering that

$$B^2 + (R_{ak} + D)^2 = R_{ja}^2 ;$$

$$B^2 = R_{ja}^2 - (R_{ak} + D)^2 ;$$

$$B^2 = (R_{ja} + R_{ak} + D)(R_{ja} - R_{ak} - D) ;$$

$$\frac{B^2}{R_{ja} + R_{ak} + D} = R_{ja} - R_{ak} - D ;$$

and

$$\frac{B^2}{R_{ja} + R_{ak} + D} + R_{ja} - R_{ak} + D = 2R_{ja} .$$

Thus, $E = 2R_{ja}$, so that one half of this result can be subtracted from $R_{ja} + R_{ak}$ to obtain the desired value of R_{ak} .

When the reports are sorted into their appropriate x_m , y_n , z_p cells, some sorting still remains to be done; some reports will certainly fit into more than one cell, because of sensor beam overlap, coarseness of the sensor beams, and uncertainty of beam orientation. In addition, it is anticipated that more than one report in a given source/sensor/beam combination may fit into a given cell. This will certainly happen if we wish to exploit the major advantage of the system--the reliance on time to determine target coordinates. This advantage allows us to achieve a system accuracy that greatly exceeds the accuracy of its components, thus minimizing the number of range cells required in each sensor.

8. DOPPLER FREQUENCY SHIFT DUE TO MOTION OF SOURCE

If the source is moving with velocity vector V , the envelope of Doppler effects comprises two spheres with their diameters lying on the velocity vector and their common point of tangency at the source (see fig. 7). Each sphere has diameter $D = V$ and represents positive or negative Doppler, respectively, as the velocity vector points toward or away from it. Diameter D is assumed small compared to the pulse repetition frequency (prf) of the source. Each sensor, to achieve coherent reception of echoes, will have the phase of its local oscillator adjusted, pulse by pulse, to match the perceived phase of the

source illumination as seen via the direct source-to-sensor path. The rate at which this phase adjustment occurs represents the component of source Doppler seen by the sensor, and the uniform phase progression experienced by the local oscillator is equivalent to a frequency shift that makes the effective frequency of the local oscillator equal to the Doppler-shifted frequency of the source as seen by the sensor.

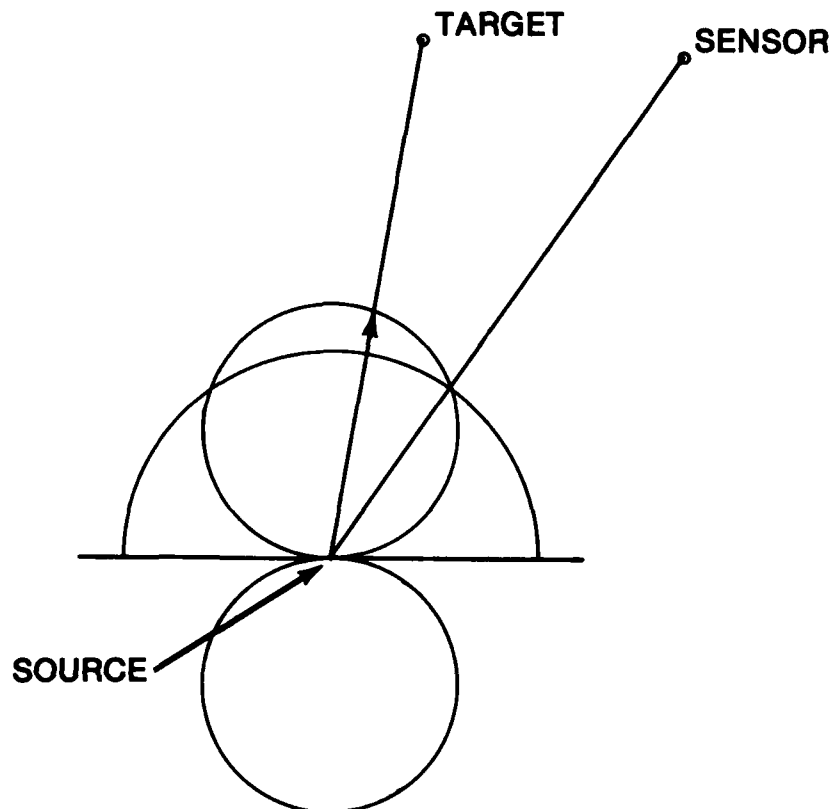


Figure 7. Doppler shifts due to motion of source.

The effect of this circumstance on the source Doppler picture can be visualized as follows:

(a) Find the "puncture point" where the source-to-sensor line of sight pierces the source Doppler envelope.

(b) Construct a hemisphere, centered at the source, with its base on the zero Doppler plane, through this puncture point.

(c) To find the source Doppler as seen by the sensor at any point, project a ray from the source to that point, and evaluate the vector length lying between the hemisphere and the original Doppler envelope, on this ray.

Doppler frequency shift due to motion of the source can be completely characterized at the system level as follows:

For each sensor, k , compute the direction cosine of R_{jk} as

$$\begin{aligned}\cos x_{jk} &= \frac{x_k - x_j}{R_{jk}} , \\ \cos y_{jk} &= \frac{y_k - y_j}{R_{jk}} , \\ \cos z_{jk} &= \frac{z_k - z_j}{R_{jk}} .\end{aligned}\tag{35}$$

The (unknown) components of the source Doppler vector D_j are D_{jx} , D_{jy} , D_{jz} .

The Doppler frequency F_{jk} observed at sensor k due to the motion of source j may be expressed as

$$F_{jk} = D_{jx} \cos x_{jk} + D_{jy} \cos y_{jk} + D_{jz} \cos z_{jk} .$$

Putting equations (35) in the matrix format, as follows,

$$\begin{vmatrix} \cos x_{j1} & \cos y_{j1} & \cos z_{j1} \\ \vdots & \vdots & \vdots \\ \cos x_{jk} & \cos y_{jk} & \cos z_{jk} \\ \vdots & \vdots & \vdots \\ \cos x_{jn} & \cos y_{jn} & \cos z_{jn} \end{vmatrix} \begin{vmatrix} D_{jx} \\ D_{jy} \\ D_{jz} \end{vmatrix} = \begin{vmatrix} F_{j1} \\ \vdots \\ F_{jk} \\ \vdots \\ F_{jn} \end{vmatrix} ,\tag{36}$$

reveals the familiar overconstrained equations, and we proceed accordingly.

The implied constraint on the system here is that the pulse rate of the source must be greater than twice the maximum Doppler because of source motion. The locus of rays that yields zero Doppler defines a cone with the vertex as the source and the axis along the source velocity vector; the sensor lies on the surface of the cone. Similarly, any locus of rays that yields a constant, nonzero Doppler defines a cone with the same vertex and axis, differing only in its apex angle.

Thus, with a high-altitude source and a sensor located on a planar terrain, elliptical (conic section, in general) isodops with the zero isodop passing through the sensor can be constructed; however, the sensor will usually lie on a major axis of its isodop. The major axes of all isodops for all source/sensor combinations will lie on the vertical projection of the source velocity vector.

All the foregoing leads to the conclusion that some sensor processors will not be operating in the best possible circumstances; this is especially so because the system design has been constrained so that no sensor has any of the analysis developed here available to it.

A numerical measure of the source Doppler as seen by each sensor can be readily generated, and these numbers can be transmitted to the central processor via the data links from each sensor to the central processor. The carrier frequency of these data links can serve as the frequency reference for the source Doppler measurements.

With the source Doppler and the source-to-sensor Doppler available in every x_n, y_u, z_p cell, their difference from the Doppler as reported on each alarm from every sensor can be constructed, thus eliminating Doppler effects due to source motion. After the alarm reports in any given cell are sorted, the velocity vector for each target in that cell can be computed, using the direction cosines of the cell-to-sensor rays and computing as was done in determining the source velocity vector.

9. DISCUSSION

It is evident that the measurable quantities in a distributed surveillance system may be regarded as projections upon a set of vectors that is established by the relative positions of the sources and/or sensors. The dimensionality of this vector space grows as we relinquish control (or absolute knowledge) of the relative timing of events within the system. It is interesting to note that lack of an absolute time

reference puts us into the spacetime geometry required by special relativity's discard of the concept of simultaneity.

Considering the spacelike coordinates alone, the relative independence among the measurements made on any target will be proportional to the size of the solid angle subtended by the source/sensor field as viewed from the target. Systems having a small solid angle are called "skew angular," since all their basis vectors are skewed from the desired mutually orthogonal directions into a single small angular spread.

The horrors of numerical operations in highly skew angular coordinates are well-established³ and can serve as a guide to deployment, with the proviso that the total spacetime interval (rather than the spacelike coordinates alone) will determine the degree of difficulty encountered in computation. The chief computation load, aside from each sensor's Doppler filtering, will reside in the target-sorting algorithms. Purely incoherent processing of sensor reports was the only technique required to establish complete analysis of system geometry; however, it should be clear that each sensor could report both amplitude and phase of target Doppler, allowing further coherent processing at the central computer.

An aspect of distributed systems whose importance cannot be overemphasized is their "distributed" redundancy and the resultant gain in reliability (or operability) that they provide. The Gaussian least-squares algorithm, if pursued to an assessment of the error vector, may be regarded as an introspective process that has miniscule probability of suffering two compensating errors that will produce wrong answers accompanied by an acceptable error vector. And it matters not where in the total system the errors occur. In the detailed discussion of the target-sorting problem, the possibility of using the compatibility condition was not mentioned, for lack of time and space. Briefly, we may state that a given combination of target reports must be orthogonal to all solutions of the adjoint homogeneous equations. An algorithm based on this condition may provide a rapid sorting technique.

10. CONCLUSION

The geometry of distributed surveillance systems is amenable to straightforward calculation in linear vector spaces of no more than five dimensions. The dimensionality of the vector space depends inversely on the knowledge (or control) of relative timing among the elements of the

³Cornelius Lanczos, *Applied Analysis*, Prentice-Hall (1957).

system. Solutions are available both for position and velocity, and angular resolution at sensors is required only to ease the target-sorting computational load. The system will fail soft, and immediately make the user aware of all but a most improbable set of errors when it fails. The systems allow a remarkable degree of autonomy to all elements, and retain the possibility of fully coherent processing of all sensor signals. Considerable further development of the concepts addressed herein will be required to establish the total feasibility of any distributed surveillance system, but the possible payoffs are

(a) totally unattended, solar-powered sensors, emplaced by helicopter on otherwise unattainable high ground, completely passive except for a low-probability-of-intercept data link, or

(b) utterly passive tanks, all sharing the same set of expendable sources, with each tank having complete knowledge of the tactical situation in coordinates centered at its own location.

ACKNOWLEDGEMENT

Numerous discussions with G. V. Cirincione of HDL, and with various other members of his Radar Technology Branch, were most helpful in raising most of the key issues that a paper of this sort should address. For anything that may have been overlooked, the authors take full responsibility.

DISTRIBUTION

ADMINISTRATOR
DEFENSE TECHNICAL INFORMATION
ATTN DTIC-DDA (12 COPIES)
CAMERON STATION, BUILDING 5
ALEXANDRIA, VA 22314

COMMANDER
US ARMY RSCH & STD GP (EUR)
ATTN CHIEF, PHYSICS & MATH BRANCH
FPO NEW YORK 09510

COMMANDER
US ARMY MISSILE & MUNITIONS
CENTER & SCHOOL
ATTN ATSK-CTD-F
REDSTONE ARSENAL, AL 35809

DIRECTOR
US ARMY MATERIEL SYSTEMS ANALYSIS
ACTIVITY
ATTN DRXSY-MP
ABERDEEN PROVING GROUND, MD 21005

DIRECTOR
US ARMY BALLISTIC RESEARCH LABORATORY
ATTN DRDAR-TSB-S (STINFO)
ABERDEEN PROVING GROUND, MD 21005

US ARMY ELECTRONICS TECHNOLOGY
& DEVICES LABORATORY
ATTN DELET-DD
FT MONMOUTH, NJ 07703

HQ, USAF/SAMI
WASHINGTON, DC 20330

TELEDYNE BROWN ENGINEERING
CUMMINGS RESEARCH PARK
ATTN DR. MELVIN L. PRICE, MS-44
HUNTSVILLE, AL 35807

ENGINEERING SOCIETIES LIBRARY
ATTN ACQUISITION DEPT
345 EAST 47TH STREET
NEW YORK, NY 10017

DIRECTOR
US ARMY SIGNALS WARFARE LABORATORY
VINT HILL FARMS STATION
ATTN ANDY LEECE (5 COPIES)
WARRENTON, VA 22186

US ARMY ELECTRONICS RESEARCH
& DEVELOPMENT COMMAND
ATTN TECHNICAL DIRECTOR, DRDEL-CT
ATTN ASSO TECH DIR R&T, DRDEL-CT-R

HARRY DIAMOND LABORATORIES
ATTN CO, MG EMMETT PAIGE, JR.
ATTN TD/TSO/DIVISION DIRECTORS
ATTN RECORD COPY, 81200
ATTN HDL LIBRARY, 81100 (2 COPIES)
ATTN HDL LIBRARY, 81100 (WOODBRIDGE)
ATTN TECHNICAL REPORTS, 81300
ATTN LEGAL OFFICE, 97000
ATTN CHAIRMAN, EDITORIAL COMMITTEE
ATTN MORRISON, R. E., 13500 (GIDEP)
ATTN JOHNSON, R. N., 15200 (5 COPIES)
ATTN DUNMORE, B. E., 15200 (5 COPIES)

3-8

DT